

# Microarray Approach for Optimizing Localized Deposition of Carbon Nanotubes Using Microhotplate Arrays

C. J. Taylor<sup>a</sup>, R. E. Cavicchi<sup>b</sup>, C. B. Montgomery<sup>b</sup>, and S. Turner<sup>a</sup>  
<sup>a</sup>Department of Chemistry, Pomona College, Claremont, CA 91711

<sup>b</sup>Chemical Science and Technology Laboratory,  
National Institute of Standards and Technology,  
Gaithersburg, MD 20899

## Abstract

A 340-element array of microhotplates was used to characterize the chemical vapor deposition growth of carbon nanotubes and nanofibers under a variety of process conditions. One dimension of the 17 by 20 element array was used to vary the thickness of a Ni catalyst layer. The second dimension was used for temperature control. Growth took place in an ambient temperature gas-flow system, with processes only occurring on activated heaters. This allowed different process sequences to be defined on different columns of the array. Four parameters were varied: pre-anneal temperature of the catalyst, the growth temperature of the carbon nanostructures, growth pressure, and growth time. Scanning electron microscope images of each array element revealed trends in microstructure as these parameters, together with catalyst thickness were varied.

Keywords: nanotube, microhotplate, chemical vapor deposition, acetylene, combinatorial

## Introduction:

In the ten years since Iijima's discovery of carbon nanotubes was reported in 1991<sup>1</sup> a vast amount of research has been performed in order to understand better carbon nanotubes (CNTs). Carbon nanotubes have interesting electrical properties and as such have broad-reaching potential applications in the fields of microelectronics, instrumentation design, and as sensors and actuators. Our interests lie in the area of gas microsensor design, where potential useful properties of CNTs include their inert surfaces, available for adsorption, and their high surface area to volume ratio. The different morphologies (straight, twisted, coiled, segmented, etc.), may be useful for producing materials with different selectivity for molecular adsorption.

Carbon nanotubes have been prepared using a variety of techniques including arc discharge<sup>2-4</sup>, laser ablation<sup>5</sup>, flame pyrolysis and chemical vapor deposition (both conventional and plasma-assisted). While it has been possible to form large quantities of CNTs using the first two methods, it has been challenging to deposit them selectively in confined areas. In addition, uniformity of the CNTs has also been difficult to control. Several reports of the use of high throughput screening methods for CNT catalyst research have been published.<sup>6-8</sup> Common to each of these approaches are combinatorial libraries of catalyst materials deposited onto some macroscale substrate. These macroscale substrates are then heated in a furnace under fixed temperature and pressure in the presence of CNT precursors. While this approach has been successful for identifying

useful catalyst compositions, the sequential nature of the thermal processing is a limiting step in the optimization of CNT processing. In this paper we report on the use of microhotplate arrays<sup>9</sup> as deposition substrates for carbon nanotube research.

We used chemical vapor deposition to deposit CNTs onto sub-100  $\mu\text{m}$  features using microhotplate arrays. Unlike other chemical vapor deposition (CVD) methods for depositing CNTs, this approach uses the microheaters embedded in the individual microhotplates as the heat source for deposition, thus allowing multiple experiments to be performed at different temperatures simultaneously. This approach is novel because, as discussed in the previous paragraph, earlier efforts in combinatorial research have been limited to operation at a single temperature and pressure.<sup>6, 7</sup> The local control of temperature makes possible sequential experiments, such as growth at different pressures or with different precursors using different elements of the array on the same substrate. Microhotplates also have short thermal time constants ( $\sim 1$  ms) and thus make it possible to probe the early stages of CNT growth with short, precisely timed deposition experiments. Important factors in chemical vapor deposition include precursor chemistry, catalyst composition and particle size,<sup>10</sup> deposition temperature, deposition pressure,<sup>11</sup> and annealing conditions used prior to CNT deposition. Depending on the conditions used, it is possible to prepare single- and multi-walled CNTs. Multiwall nanotubes (MWNTs) may be completely open on the inside or segmented (bamboo).<sup>4, 12</sup> It is also possible to prepare solid carbon nanofilaments (CNFs).<sup>13</sup>

## **Experiment:**

In order to examine in an efficient manner the parameters known to effect CNT formation, experiments were performed using a 340-element microhotplate array. Figure 1 illustrates the configuration of the array. Nickel was used as the catalyst. The array was prepared for deposition by sequential masking of two rows of 20 elements at a time and sputtering the Ni catalyst using a DC magnetron sputtering system (AJA Rapier 100<sup>14</sup>). Catalyst thicknesses ranged from 2.7 nm to 90 nm. Following deposition of the catalyst layer, samples were pre-annealed in the sputtering system for 20 minutes at  $\sim 10^{-5}$  Pa. Following annealing, the sample was transferred to the deposition system for CNT deposition. The system is essentially a high-temperature glass tube with gas inlets, connected to a mechanical vacuum pump. Gas flows are controlled by three MKS 1259C mass flow controllers and an MKS 647 B mass flow programmer/display<sup>14</sup>. After transferring the completed array to the CNT deposition system, the samples were annealed at 465  $^{\circ}\text{C}$  in a 50:50  $\text{H}_2$ :Ar ambient at atmospheric pressure for 2-3 minutes to reduce any surface oxide formed during the transfer of the samples and to roughen the surface.

The plan of growth experiments using the array is indicated in Figure 2. Two sets of growth experiments were conducted. The first set, at atmospheric pressure, used 10 rows of the array, and the second set at 4 Pa was performed on 8 rows. Two rows were unused. Between the two growths and after the final growth, the sample was examined with scanning electron microscopy (SEM). For a limited number of elements we were able to

transfer some of the CNT material from a microhotplate to a transmission electron microscopy (TEM) grid using the probes of a micromanipulator. Occasionally this procedure resulted in the breakage of the fragile microhotplate.

#### Atmospheric pressure deposition experiments:

In the first set of experiments, four different pre-annealing and deposition temperatures were used ( $465\pm 5$ ,  $520\pm 8$ ,  $670\pm 20$  and  $770\pm 30$  °C with deposition temperatures based on calibrated resistance change in the heater). The deposition temperatures were not allowed to exceed the pre-anneal temperature. During deposition the pressure was held at 1 atm and growth times were all 20 minutes. A 50:50 argon:acetylene mixture was used for CNT growth. Following CNT deposition on all 10 columns, the array was transferred to the SEM (Hitachi S-4100<sup>14</sup>) for evaluation (30 kV, 9 mm working distance). Even prior to SEM analysis, it was immediately apparent even using a magnifying glass that a significant amount of material had been deposited onto many of the elements. Since all but one of the catalyst thicknesses were prepared in duplicate, it was possible to evaluate reproducibility of our process. Figure 3 shows an example of the coverage of CNTs typical for these experiments.

#### Reduced pressure deposition experiments:

Two types of experiments were performed at reduced pressure (4 Pa). The first mirrors the atmospheric pressure depositions with a constant annealing temperature and a 20 minute deposition time. The second type of experiment uses the highest annealing temperature, a lower deposition temperature and deposition times from 12 seconds to 20 minutes. This latter experiment is made possible by the microhotplates' short thermal time constants which provide on/off switching on the order of 1-2 milliseconds. Deposition experiments were performed to examine how the flux of carbon to the growing CNT affected the morphology and the density of the deposits. Atmospheric pressure deposition resulted in a mixture of helical and straight carbon deposits. Transmission electron micrographs obtained from samples prepared in an earlier experiment conducted on a smaller microhotplate array indicated that the straight deposits are nanotubes with the bamboo morphology as shown in Figure 4 (a) while the helical deposits are filamentous in nature.

### **Results and discussion:**

Tip catalyzed growth is the common growth mode for Ni-seeded growth.<sup>15</sup> Figure 4 (b) shows a TEM image in which the dark area at the end of the nanofiber was identified by energy dispersive X-ray spectroscopy to be a Ni particle.

A broad range of morphologies was observed over the range of deposition parameters used for the different array elements. The thinnest catalyst layer (2.7 nm) yielded the most uniform deposits. Other catalyst thicknesses were also successful in enabling the growth of CNTs, but with a variety of diameters and morphologies, indicating possible

differences in the growth mode from the catalyst film. Figure 5 illustrates the change in morphology with increasing deposition temperature for samples prepared at the highest annealing temperature. It appears as though the increase in deposition temperature increases the amount of amorphous carbon deposited as well.

Increasing the catalyst thickness broadened the distribution of CNT diameters and introduced helical filamentary carbon. Figure 6 compares the growth of carbon nanostructures for two thicknesses of Ni catalyst. For the thicker catalyst layer, we observe carbon nanotubes or nanofibers with larger diameters and a broader distribution of diameters. The observations are consistent with other work showing that thicker catalyst layers produce larger diameter CNTs.<sup>16,17</sup> Also, the thicker layer corresponds to a size regime in which the shape of small metal particles begin to adopt distinct “crystal habit,” compared to the spheroid shapes of smaller particles.<sup>18</sup> This may also influence the kind of carbon nanostructures that can form.

Previous work in this area suggests that there is a relationship between the helical coils of carbon and defects in the structure.<sup>19,20</sup> When the kinetics are favorable for the preparation of hexagonal sub-units, the morphology is straight, however, there are also conditions such as high flux, where the kinetics favor a coiled product. Consistent with this hypothesis were the results from a comparison of the effect of growth pressure, as demonstrated in Figure 7. Samples prepared under atmospheric pressure processing temperatures were found to catalyze the growth of large amounts of coiled products, while at 4 Pa there was a dramatic decrease in the amount of coiled deposits.

The images in Figure 8 compare growth times of duration 12 s and 20 min. For catalyst thicknesses of 2.7 nm and 9.0 nm we observe both CNT structures and carbon-coated metal particles. For the 2.7 nm thick catalyst, the observation of CNTs of comparable length for the two growth times suggests the growth of individual CNTs is rapid but may terminate. This result has motivated studies of shorter growth times, down to the millisecond timescale using microhotplates, which are underway. The major differences evident here between the two growth times are the appearance of longer, larger diameter tubes for the 9.0 nm thick catalyst, and the increasing thickness of amorphous carbon surrounding metal particles for both the 9.0 nm and 90 nm thick catalysts. This suggests that larger tubes grow more slowly, and that the fraction of amorphous carbon increases with time.

## **Conclusion:**

We have demonstrated the use of microhotplate arrays for the combinatorial optimization of processing parameters in CNT synthesis. The distinct advantage presented of using microhotplate arrays is the local control of temperature, allowing the comparison of different processing sequences on each element. We are currently expanding this research to further explore the use of this type of approach for catalyst optimization and incorporation of CNTs into mixed sensor arrays both as the sensing element and as gas preconcentrators. This approach should enable fast screening of processing parameters in the preparation of CNT films.

**Acknowledgements:**

The authors acknowledge the partial support of the Department of Energy Grant #07-98ER62709. Dr. Taylor would also like to acknowledge the support of the National Research Council-National Institute of Standards and Technology Postdoctoral Research Associateship Program.

## Figure Captions:

Figure 1. Composite optical micrograph (large image) and SEM (smaller inset) image and of a 340-element array similar to the one used in this experiment. Also shown is higher magnification image of a single microhotplate complete with buried serpentine polysilicon heater.

Figure 2. Schematic diagram summarizing the details of this set of experiments.

Figure 3. Scanning electron micrograph of two adjacent microhotplates illustrating the coverage of CNTs as well as the slight differences in the total amount of material deposited. The microhotplate on the right was operated at 670 °C while the hotplate on the left was operated at 520 °C. Closer inspection of these samples also revealed a larger proportion of coiled material on the microhotplate operated at the lower temperature. Note, the asymmetric shape of the deposit is due to the shape of the mask.

Figure 4. Transmission electron micrographs of a filament deposited on 18nm Ni at 520 °C and subsequently transferred to a TEM grid. Energy dispersive spectroscopy (EDS) was used to show that the dark area at the end is Ni.

Figure 5. Scanning electron micrographs of CNT material deposited on 2.7nm Ni at 465 °C, 520 °C, 670 °C and 770 °C following a 770 °C annealing step.

Figure 6. Scanning electron micrographs demonstrating the differences in CNT uniformity observed at two different Ni catalyst thicknesses A 2.7 nm and B 18 nm. Both samples were deposited at 465 °C at atmospheric pressure.

Figure 7. Scanning electron micrographs demonstrating the effect of growth pressure on microstructure. The Ni thickness was 13.5 nm for both devices. The carbon material in (A) was deposited at  $10^5$  Pa and the material in (B) was deposited at 4 Pa. Both samples were deposited at 520 °C following an annealing step at the same temperature.

Figure 8. Scanning electron micrographs comparing 12 second deposition (left) and the 20 minute deposition (right) for catalyst thicknesses of 2.7 nm, 9.0 nm and 90 nm, increasing from top to bottom.

## References:

- (1) Iijima, S. *Nature* **1991**, *354*, 56-58.
- (2) Iijima, S. *Materials Science and Engineering B-Solid State Materials for Advanced Technology* **1993**, *19*, 172-180.
- (3) Smalley, R. E. *Materials Science and Engineering B-Solid State Materials for Advanced Technology* **1993**, *19*, 1-7.
- (4) Saito, Y.; Yoshikawa, T.; Okuda, M.; Fujimoto, N.; Sumiyama, K.; Suzuki, K.; Kasuya, A.; Nishina, Y. *Journal of Physics and Chemistry of Solids* **1993**, *54*, 1849-1860.
- (5) Guo, T.; Nikolaev, P.; Thess, A.; Colbert, D. T.; Smalley, R. E. *Chemical Physics Letters* **1995**, *243*, 49-54.
- (6) Klinke, C.; Bonard, J. M.; Kern, K. *Surface Science* **2001**, *492*, 195-201.
- (7) (Cassell, A. M.; Verma, S.; Delzeit, L.; Meyyappan, M.; Han, J. *Langmuir* **2001**, *17*, 260-264.
- (8) Chen, B.; Parker, G.; Han, J.; Meyyappan, M.; Cassell, A. M. *Chemistry of Materials* **2002**, *14*, 1891-1896.
- (9) Suehle, J. S.; Cavicchi, R. E.; Gaitan, M.; Semancik, S. *IEEE Electron Device Letters* **1993**, *14*, 118-120.
- (10) Kibria, A.; Mo, Y. H.; Nahm, K. S.; Kim, M. J. *Carbon* **2002**, *40*, 1241-1247.
- (11) Li, W. Z.; Wen, J. G.; Ren, Z. F. *Applied Physics a-Materials Science & Processing* **2002**, *74*, 397-402.
- (12) Endo, M.; Takeuchi, K.; Igarashi, S.; Kobori, K.; Shiraishi, M.; Kroto, H. W. *Journal of Physics and Chemistry of Solids* **1993**, *54*, 1841-1848.
- (13) Kim, M. S.; Rodriguez, N. M.; Baker, R. T. K. *Journal of Catalysis* **1991**, *131*, 60-73.
- (14) "Certain commercial instruments are identified to adequately specify the experimental procedure. In no case does such identification imply endorsement by the national institute of standards and technology."
- (15) Z. P. Huang, D. Z. Wang, J. G. Wen, M. Sennett, H. Gibson and Z. F. Ren, *Appl. Phys. A*. **2002**, *74* 387-391.
- (16) Cheung, C. L.; Kurtz, A.; Park, H.; Lieber, C. M. *Journal of Physical Chemistry B* **2002**, *106*, 2429-2433.
- (17) Kukovitsky, E. F.; L'Vov, S. G.; Sainov, N. A.; Shustov, V. A.; Chernozatonskii, L. A. *Chemical Physics Letters* **2002**, *355*, 497-503.

- (18) C.G. Granqvist and R. A. Buhrman, *J. Applied Phys.*, 1976, 47, 2200-2219.
- (19) Fonseca, A.; Hernadi, K.; Nagy, J. B.; Lambin, P.; Lucas, A. A. *Synthetic Metals* **1996**, 77, 235-242.
- (20) Owens, W. T.; Rodriguez, N. M.; Baker, R. T. K. *Catalysis Today* **1994**, 21, 3-22.

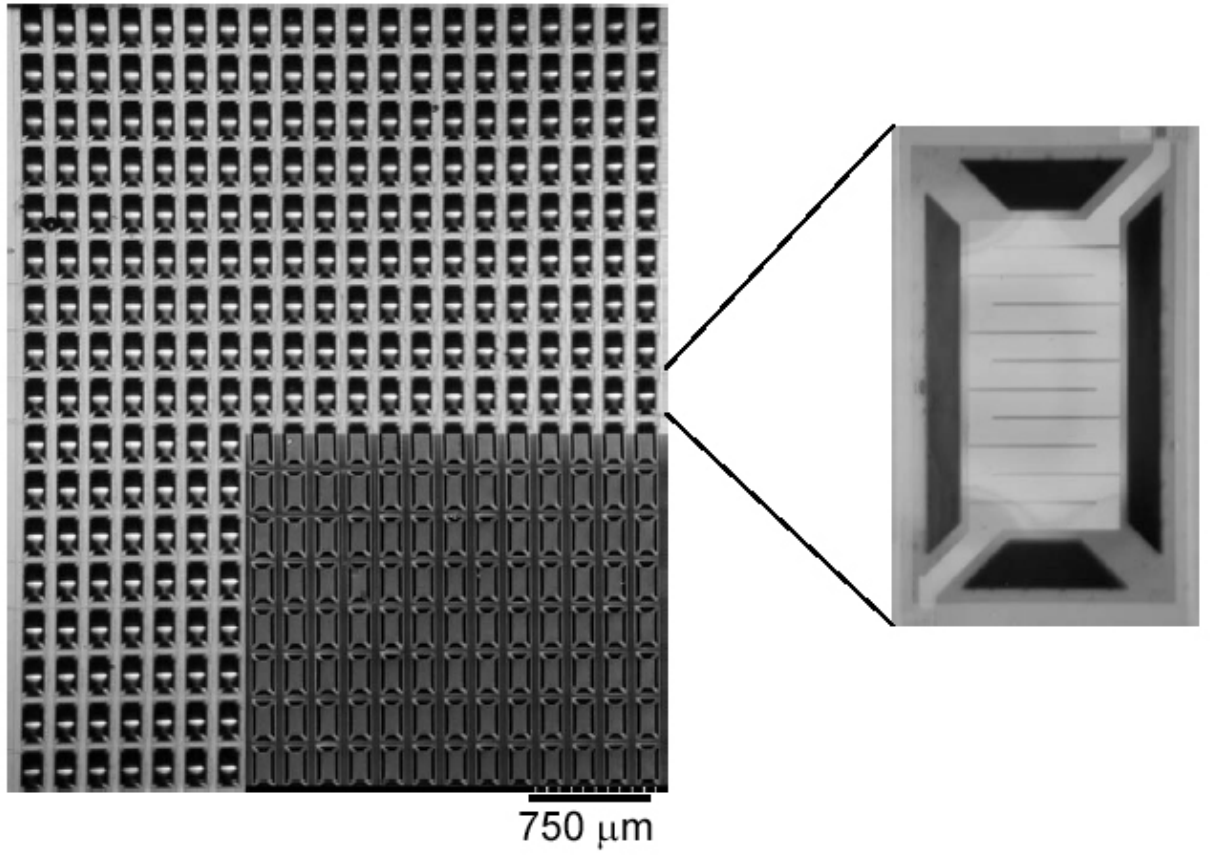


Figure 1.

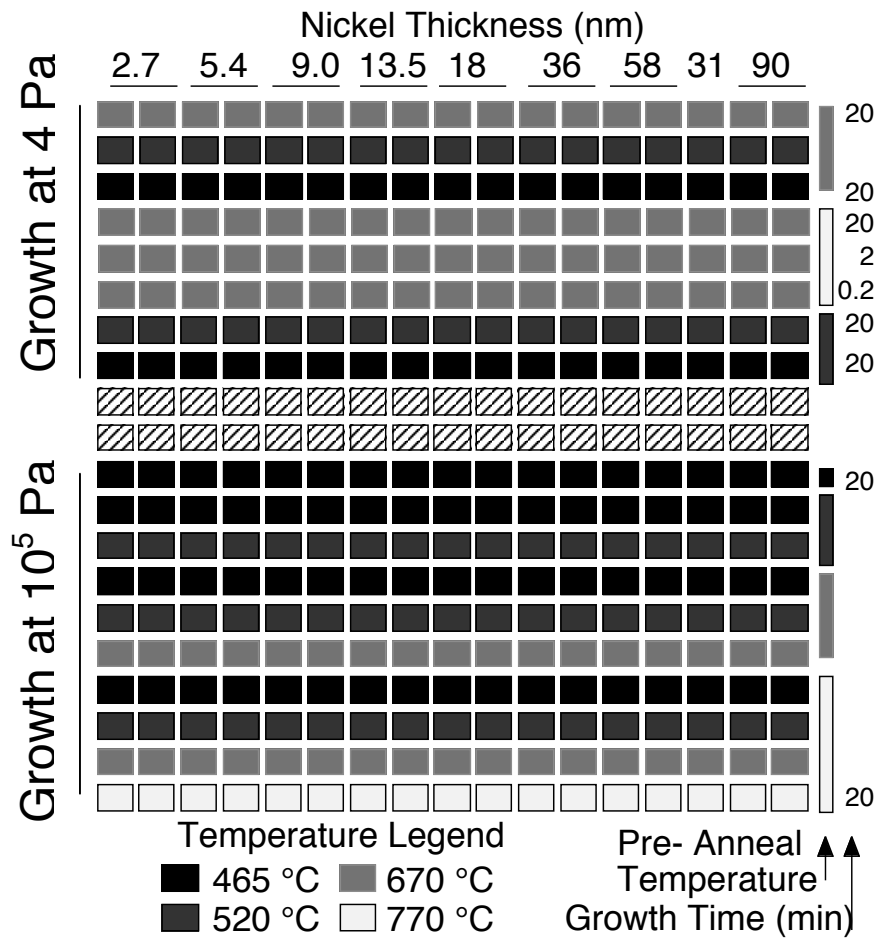


Figure 2.

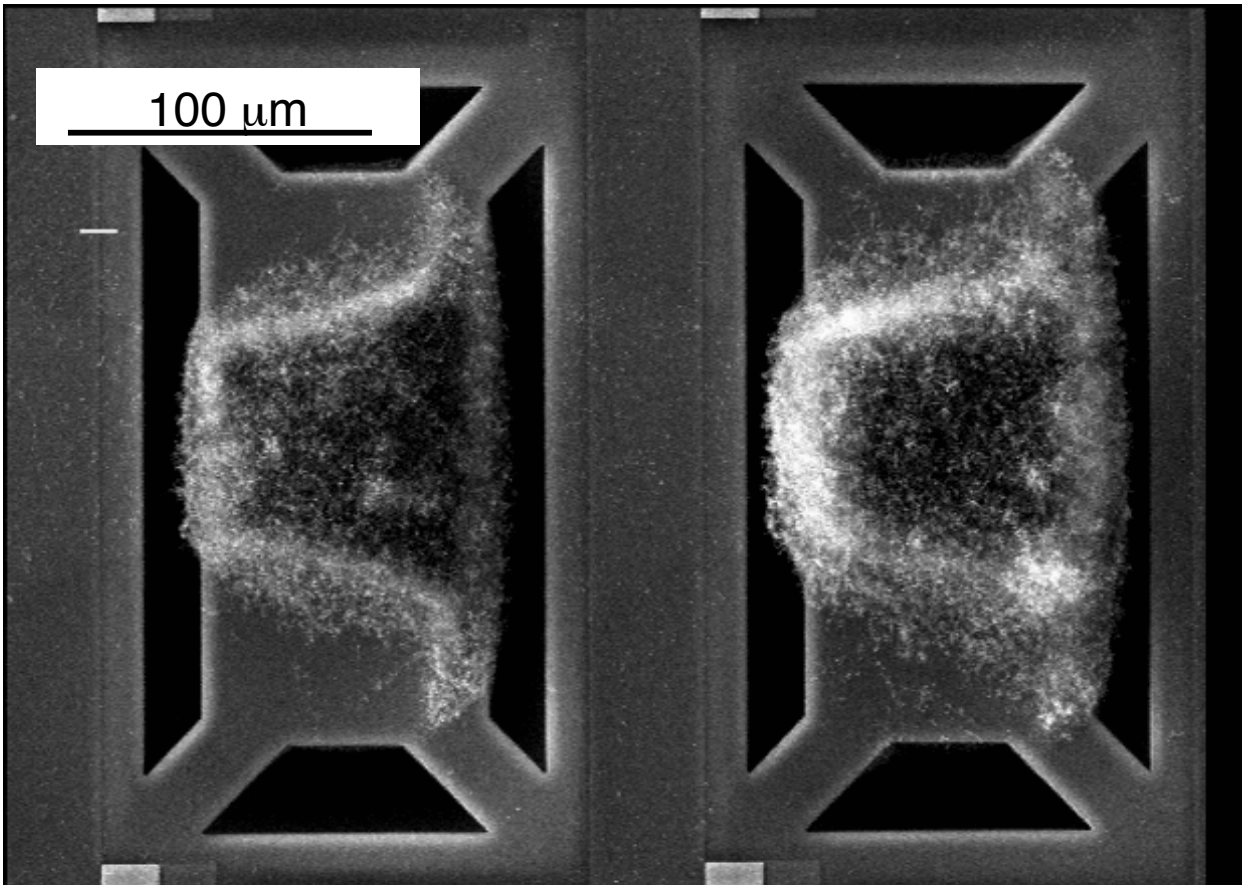


Figure 3.

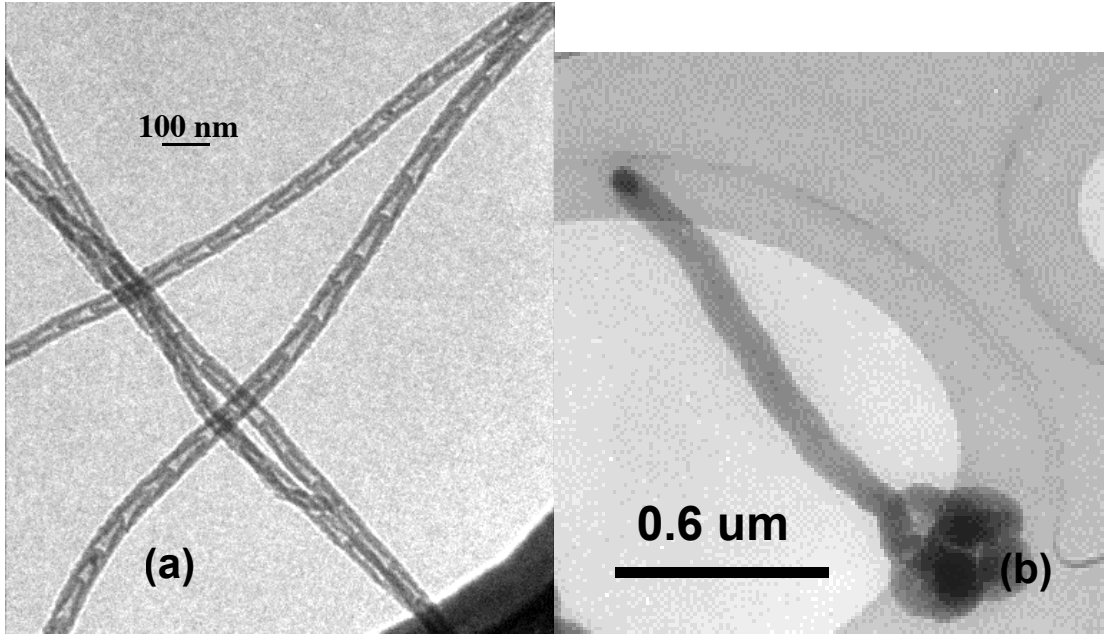


Figure 4.

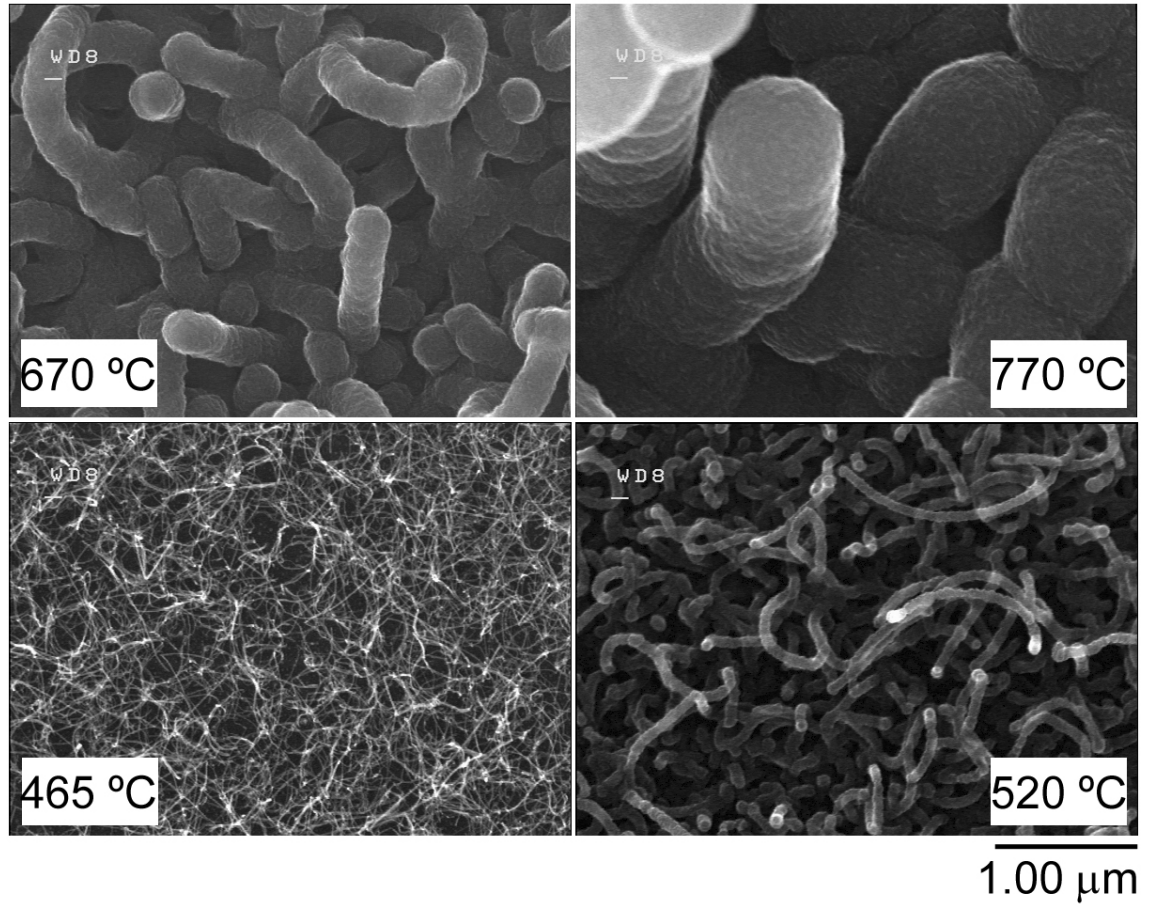


Figure 5.

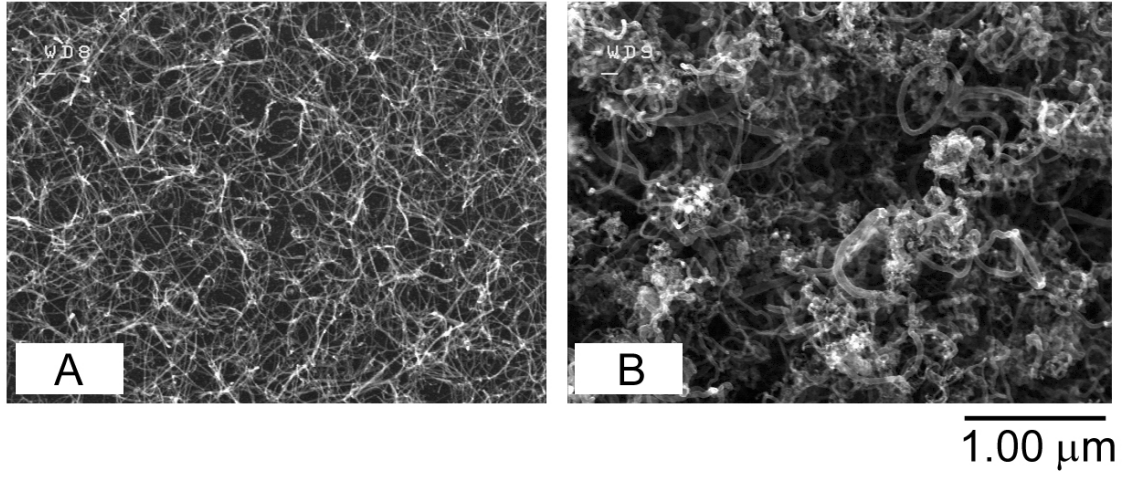


Figure 6.

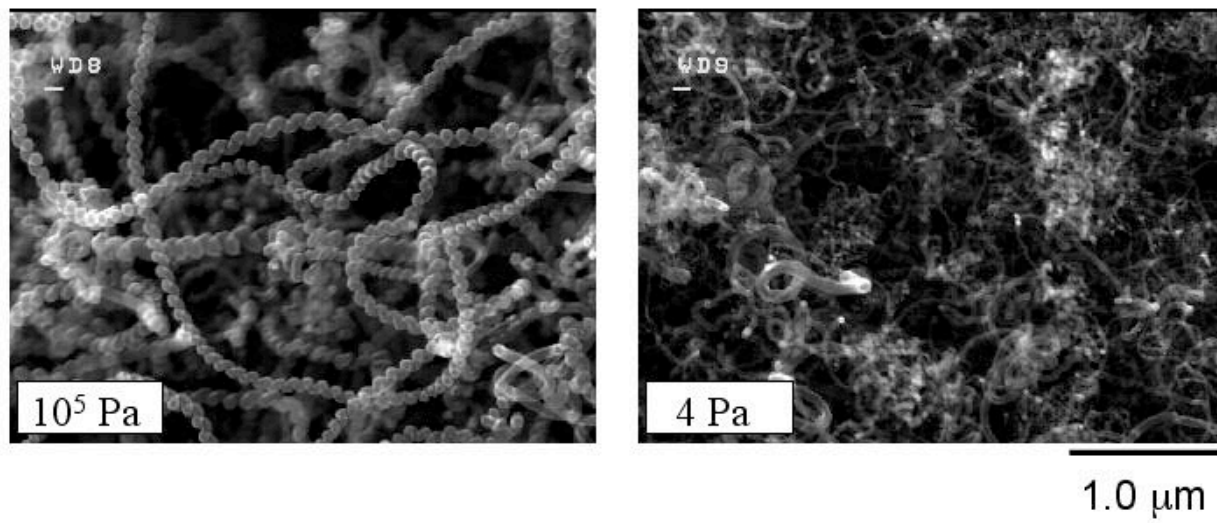


Figure 7.

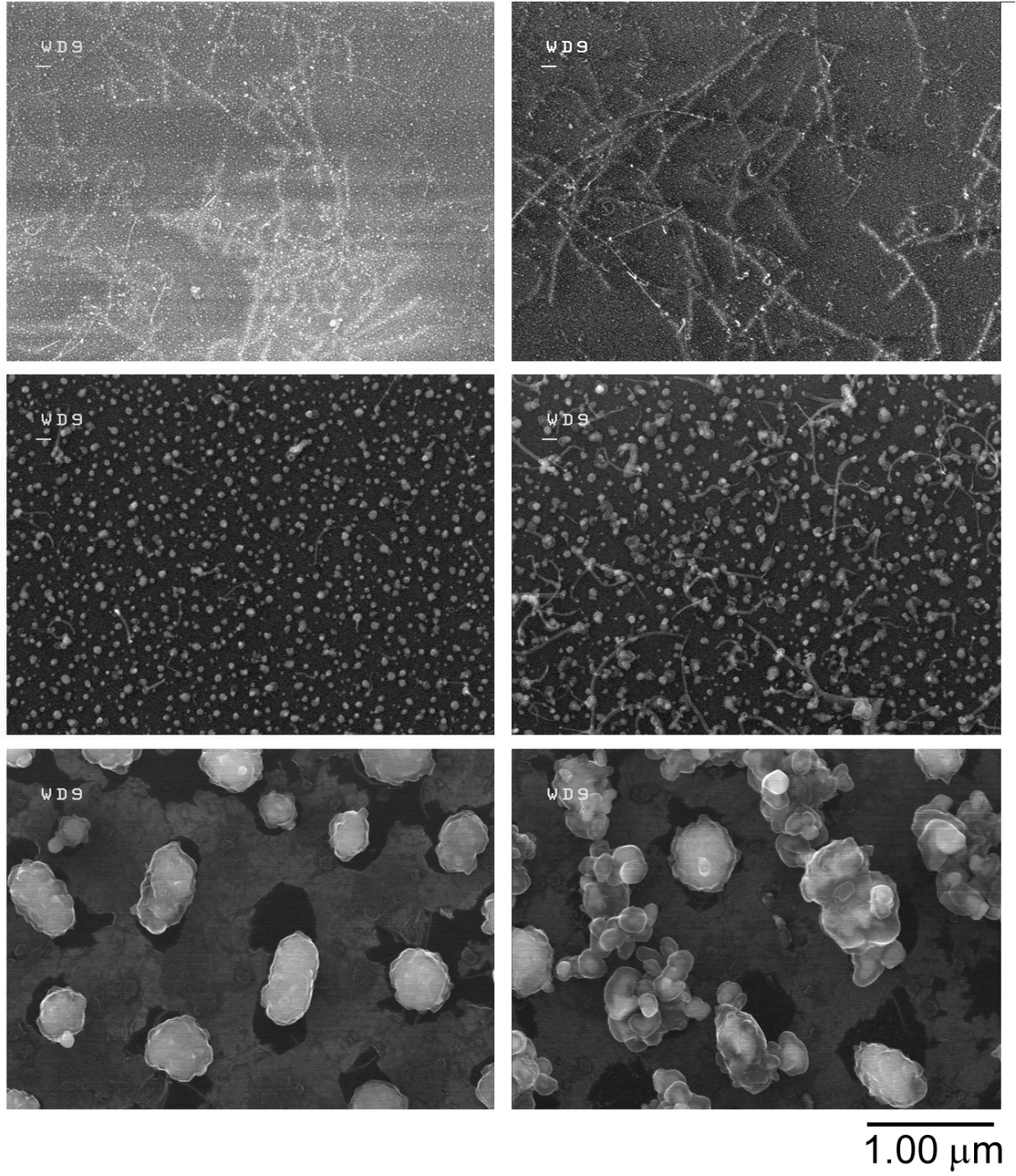


Figure 8.